

# Reconfigurable Fault Tolerant Control Using GIMC Structure \*

Daniel U. Campos Delgado  
College of Sciences  
UASLP  
Mexico  
ducd@galia.fc.uaslp.mx

Kemin Zhou  
Dept. of Elec. & Comp. Eng.  
Louisiana State University  
Baton Rouge, Louisiana 70803, USA  
kemin@ee.lsu.edu

September 11, 2002

## Abstract

In this note, a fault-tolerant control strategy is proposed from a robust control perspective by applying the recently introduced GIMC (Generalized Internal Mode Control) architecture. This fault-tolerant control design consists of two parts: a nominal performance controller and a robustness controller, and works in such way that when a sensor failure is detected, the controller structure is reconfigured by adding a robustness loop to compensate the fault. This note shows how to design such controllers for a single-input two-output gyroscope system so that the performance with the nominal controller may be maintained in the case of sensor failure and/or model uncertainties.

## 1 Introduction

Keeping good performance in the event of sensor/actuator failures are crucial in many applications, especially if costly equipments are controlled. Consequently, fault detection and fault tolerant control have become very active research topics in recent years. The main challenge in the fault detection field is to develop detection algorithms that could distinguish between faults and disturbances into the system or model uncertainties [2, 3]. Thus, filters are designed such that the effect of faults is maximized while the effect of disturbances is minimized. Several approaches have been suggested: robust detection and isolation based on eigenstructure assignment [14], estimation based on  $H_2$  and  $H_\infty$  optimization [4, 12], detection and isolation by frequency domain optimization [7, 13], detection based on model-based probabilistic approaches [6], etc. Most of the existing research is focused on linear systems, but extensions to fault detection and isolation of nonlinear systems have also been proposed in [5] and [8]. Furthermore, the applications of fuzzy logic [1] and wavelet transforms [17] to fault detection have been recently introduced.

One way of synthesizing fault-tolerant controllers is by appealing to  $H_\infty$  robust design techniques [2, 9, 19]. Unfortunately, the standard  $H_\infty$  based robust control design is based on the worst case scenario which may never occur and it is not surprising to see that such a control system does not perform very well even though it is robust to model uncertainties and sensor faults. On the other hand, reconfigurable fault tolerant structures have also been studied where the model-matching strategy is used to design linear [16] and nonlinear [10] controllers. In [11], a fault-tolerant strategy

---

\*This research is supported in part by grants from AFOSR (F49620-99-1-0179), NASA (NCC5-573), LEQSF (NASA/LEQSF(2001-04)-01), CONACYT(C01-FRC-12.22) and FAI(C01-FAI-11-8.91).

was suggested based on actuator and sensor fault compensations for a winding machine. The problem of adaptive compensation for actuator failures was recently addressed in [15].

Motivated from the design limitations of  $H_\infty$  techniques, one of the authors has recently introduced a new controller architecture in [18], called *Generalized Internal Model Control* (GIMC), which can overcome the classical conflict between performance and robustness in the traditional feedback framework. This controller architecture uses the well-known Youla controller parameterization in a completely different way. First of all, a high performance controller, say  $K_0$ , can be designed using any standard method, and then a robustification controller, say  $Q$ , can be designed to guarantee robust stability and performance using any robust control techniques. The feedback control system will be solely controlled by the high performance controller  $K_0$  in the normal case and the robustification controller  $Q$  will only be active when there is a sensor fault or external disturbances. In this paper, we shall test this GIMC control strategy on a gyroscope experiment in our lab.

The paper is organized as follows. Section 2 describes the philosophy behind the GIMC architecture. The details about the fault compensation strategy are shown in Section 3. Section 4 gives a description of the setup of the gyroscope experiment. In section 5, the GIMC controller is designed and implemented for the gyroscope experiment. Both numerical simulation and experimental results are reported. Section 6 gives some concluding remarks.

## 2 GIMC for Fault Tolerant Control

Let  $P_0$  be a nominal model of the linear plant  $P$  and  $K_0$  be a linear stabilizing controller for  $P_0$ . Suppose that  $K_0$  and  $P_0$  have the following coprime factorizations

$$K_0 = \tilde{V}^{-1}\tilde{U}, \quad P_0 = \tilde{M}^{-1}\tilde{N}.$$

Then every controller  $K_0$  that internally stabilizes  $P_0$  can be written in the following form:

$$K = (\tilde{V} - Q\tilde{N})^{-1}(\tilde{U} + Q\tilde{M})$$

for some  $Q \in H_\infty$  such that  $\det(\tilde{V}(\infty) - Q(\infty)\tilde{N}(\infty)) \neq 0$ , see [19].

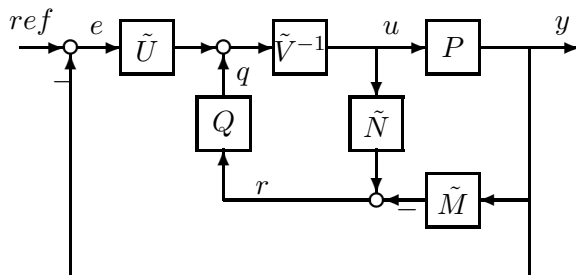


Figure 1: Generalized internal model (GIMC) control structure.

A new implementation of the controller parameterization called *Generalized Internal Mode Control* (GIMC) is proposed in [18] as shown in Figure 1. Note that

$$r(s) = \tilde{N}(s)u(s) - \tilde{M}(s)y(s)$$

Hence  $r$  is the error between the estimated output and the true output of the system (residual signal) [2]. Thus  $r = 0$  if there is no model uncertainties, external disturbances or faults and then

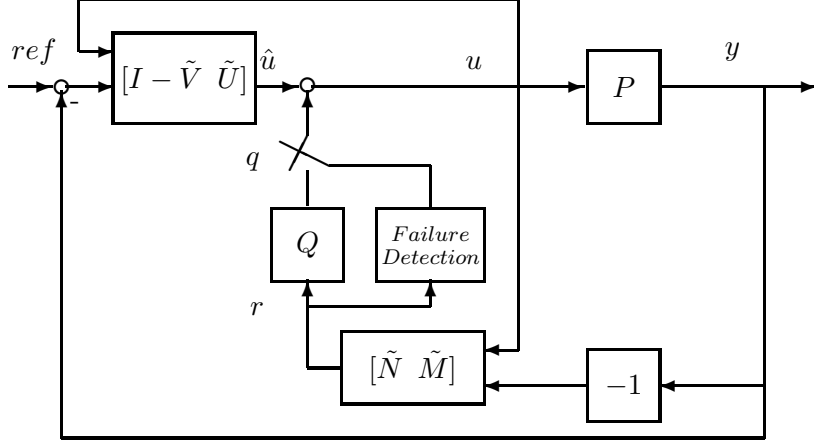


Figure 2: GIMC structure with failure detector.

the control system will be solely controlled by the high performance controller  $K_0 = \tilde{V}^{-1}\tilde{U}$ . On the other hand, the robustification controller  $Q$  will only be active when  $r \neq 0$ , i.e., there are either model uncertainties or external disturbances or sensor/actuator faults.

Since the signal  $r$  represents the estimated output error (residual), this signal contains valuable information in case of a sensor failure. Consequently, in order to have the exact nominal performance in case of no-failure,  $r$  could be monitored to detect a sensor or actuator failure and then activate the robustness loop, i.e. switch on the signal  $q$ . Thus, the GIMC structure can also be implemented as shown in Figure 2. This will improve the performance of the overall GIMC structure, since there is no degradation of nominal performance in order to improve robustness.

### 3 Fault Compensation

In general, the sensor and actuator faults can be modeled in a multiplicative form

$$\begin{aligned}\hat{y}(s) &= [I + \Delta_s]y(s) \\ \hat{u}(s) &= [I + \Delta_a]u(s)\end{aligned}$$

where  $\Delta_s, \Delta_a \in H_\infty$  represent the sensor and actuator perturbations due to the faults. Consequently, if these terms are appended to the nominal plant  $P_0$ , then the faulted input-output mapping  $P(s)$  can be represented as

$$\begin{aligned}P(s) &= P_0[I + \Delta_a] \quad (\text{actuator fault}) \\ P(s) &= [I + \Delta_s]P_0 \quad (\text{sensor fault})\end{aligned}\tag{1}$$

Thus the sensor or actuator fault can be modeled as model uncertainties. As a result, we consider the following general class of uncertain models

$$P = P_0 + W_1\Delta W_2\tag{2}$$

where  $P_0$  is the nominal plant,  $\Delta \in H_\infty$  is an uncertainty block such that  $\|\Delta\|_\infty \leq 1$ ,  $W_1$  and  $W_2$  are uncertainty weights such that  $P$  and  $P_0$  have the same number of unstable poles for all allowable  $\Delta$ . For example,  $P = (I + \Delta)P_0$  with  $W_1 = P_0$  and  $W_2 = I$  may represent the sensor

failures with  $\Delta = -I$  characterizing the lack of all sensor measurements and  $P = P_0(I + \Delta)$  with  $W_1 = I$  and  $W_2 = P_0$  may represent actuator failures. Note that with this formulation, disturbances could also be considered as faults. However, it is assumed that the fault detection scheme can distinguish between disturbances and actual faults. In fact, this is feasible if some knowledge about the frequency information of the faults and external disturbances is previously known [7, 13].

We shall consider a basic robustness requirement in this paper, i.e. the closed-loop stability. Hence our objective is to design  $Q$  to maximize the failure tolerance in the closed-loop system, i.e.

$$\min_Q \|T_{zw}\|_\infty \quad (3)$$

where  $T_{zw}$  is the closed-loop transfer function from signals  $w$  to  $z$ , see Figure 3. Fortunately, this problem has an obvious answer if  $P_0 \in H_\infty$ .

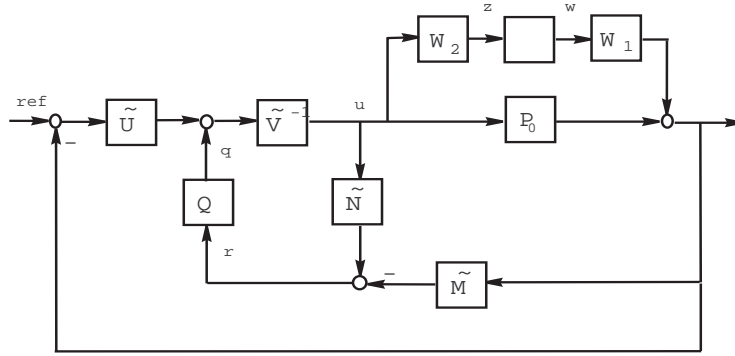


Figure 3: Gimc Architecture with Uncertain Plant.

**Theorem 1** Suppose  $W_1, W_2 \in H_\infty$ ,  $P_0 \in H_\infty$  and  $K_0 = \tilde{V}^{-1}\tilde{U}$  is a stabilizing controller of  $P_0$  that satisfies the closed-loop performance requirements, then

$$Q = -\tilde{U}\tilde{M}^{-1} \quad (4)$$

is the optimal solution to the optimization problem  $\min_Q \|T_{zw}\|_\infty$ . Moreover, if  $Q$  is chosen in this way,  $\|T_{zw}\|_\infty = 0$ , the closed-loop transfer function from  $ref$  (reference) to  $u$  (control signal) is given by

$$T_{uref} = (I + K_0P_0)^{-1}K_0. \quad (5)$$

*Proof:* From Figure 3, it can be seen that (with  $ref = 0$ )

$$u(s) = \tilde{V}^{-1} \left[ -\tilde{U} \{W_1w(s) + P_0u(s)\} + Q \left( \tilde{N}u(s) - \tilde{M}\{W_1w(s) + P_0u(s)\} \right) \right]$$

and  $z(s) = W_2u(s)$ . Therefore, since  $P_0 = \tilde{M}^{-1}\tilde{N}$  and after some simplification

$$T_{zw} = -W_2[I + K_0P_0]^{-1}\tilde{V}^{-1}[\tilde{U} + Q\tilde{M}]W_1 \quad (6)$$

Consequently, the optimal solution to the robust stability problem is

$$\min_Q \|T_{zw}\|_\infty = 0, \quad Q = -\tilde{U}\tilde{M}^{-1}$$

since  $\tilde{M}^{-1} \in H_\infty$ . Next, note that

$$u(s) = \tilde{V}^{-1} \left[ \tilde{U} (ref(s) - Pu(s)) + Q (\tilde{N}u(s) - \tilde{M}Pu(s)) \right]$$

with  $Q = -\tilde{U}\tilde{M}^{-1}$  and after some calculations and simplifications, we have

$$u(s) = \tilde{V}^{-1}\tilde{U}ref(s) - \tilde{V}^{-1}\tilde{U}\tilde{M}^{-1}\tilde{N}u(s)$$

Therefore,  $T_{uref} = [I + K_0P_0]^{-1}K_0$  since  $K_0 = \tilde{V}^{-1}\tilde{U}$ .

□

Thus, if the  $q$  signal is introduced into the closed-loop, the control system is equivalent to running in an open loop with a reference  $ref$  and an open-loop controller  $K = [I + K_0P_0]^{-1}K_0$ . Of course, this will not be the case if additional performance criteria are included in the  $H_\infty$  design.

On the other hand, if the plant  $P_0$  is not stable, then a weighted  $H_\infty$  approximation has to be solved, as it is seen from (6). Moreover, this problem can be put in an LFT framework, as seen in Figure 4, with the generalized plant  $G$  given by

$$G = \begin{bmatrix} -W_2SK_0W_1 & W_2S\tilde{V}^{-1} \\ -\tilde{M}W_1 & 0 \end{bmatrix} \quad (7)$$

where  $S = (I + K_0P_0)^{-1}$ . Hence,  $Q$  is chosen according to

$$\gamma = \min_Q \|\mathcal{F}_l(G, Q)\|_\infty \quad (8)$$

and internal stability is guaranteed if  $\|\Delta\|_\infty < 1/\gamma$ . Alternatively, if an output uncertainty (sensor fault) is considered for the unstable plant  $P_0$ , i.e.  $P = (I + \Delta)P_0$ . The generalized plant  $G$  will now be given by

$$G = \begin{bmatrix} -\tilde{S}P_0K_0 & \tilde{S}P_0\tilde{V}^{-1} \\ -\tilde{M} & 0 \end{bmatrix} \quad (9)$$

where  $\tilde{S} = (I + P_0K_0)^{-1}$ . Note that in this case  $\gamma \geq 1$  since this will represent that the maximum tolerable uncertainty is always  $\|\Delta\|_\infty < 1$ . Otherwise, the uncertainty could take the value  $\Delta = -I$  (sensors outage) and the closed-loop will become unstable.

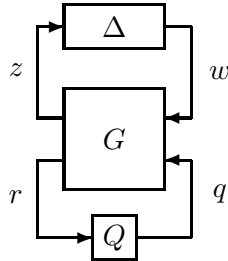


Figure 4: Generalized linear fractional transformation.

We want to point out that it may not always be desirable to have the compensation signal  $q$  active all the time if  $P_0$  is stable and the controller  $Q$  in Theorem 1 is used. This is because in this case the control system will operate in an open-loop fashion with an equivalent open-loop controller  $[I + K_0P_0]^{-1}K_0$  and the system performance has no tolerance to disturbances and model

mismatches. Consequently, it is recommended to adopt the controller structure in Figure 2 where the compensation signal  $q$  is introduced only when a sensor failure is detected.

It is important to mention that with the configuration of Figure 2, the closed-loop system is not linear time-invariant anymore. So, it is natural to ask about the stability of the overall closed-loop with this scheme. However, note that once a fault is detected, the switch is activated and the compensation signal  $q$  enters into the system and remains active until the proper sensor replacement is done. Consequently, the switching is performed only once during the system operation. Thus, the signal  $q$  is not continuously switched on and off. Therefore, if there exists a  $\Delta \in H_\infty$  such that  $T_{yr} \notin H_\infty$ , after the fault is detected and  $q$  is activated, the closed-loop will be stable again if  $P_0 \in H_\infty$  and  $Q$  is selected according to (4). For  $P_0 \notin H_\infty$ , the closed-loop stability is again recovered if  $\|\Delta\|_\infty < 1/\gamma$  and  $Q$  satisfies (8).

## 4 Experiment Description

The fault tolerant structure will now be tested in a MIMO gyroscope experiment. The plant, shown in Figure 5, consists of a high inertia brass rotor suspended in an assembly with four angular degrees of freedom. The rotor spin torque is provided by a DC motor (motor #1). The first transverse gimbal assembly (body C) is driven by another DC motor (motor #2) to effect motion about axis 2. Both motors have restrictions on rotation rates to commands change, which are represented by saturations of  $\pm 10V$  in their input voltages. In this paper, we shall consider a special case where

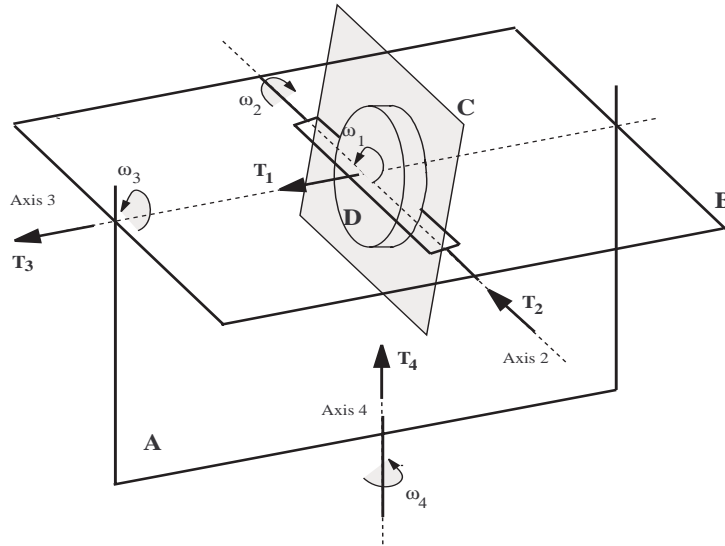


Figure 5: A gyroscope system.

the gimbal axis 3 is locked so that bodies A and B become one rigid body. The resulting plant is useful for demonstrations of gyroscopic torque action where the position and rate,  $q_4$  and  $\omega_4$ , may be controlled by rotating gimbal #2,  $q_2$ , while the rotor is spinning. Taking the coordinate frame definition from Figure 5, a nonlinear model can be obtained. A linearized version around the origin

can be derived as follows:

$$\dot{\mathbf{x}} = \begin{bmatrix} 0 & 0 & 1 \\ 0 & 0 & \frac{J_D \Omega}{I_C + I_D} \\ 0 & \frac{-J_D \Omega}{I_D + K_A + K_B + K_C} & 0 \end{bmatrix} \mathbf{x} + \begin{bmatrix} 0 \\ \frac{1}{I_D + I_C} \\ 0 \end{bmatrix} T_2$$

$$\begin{bmatrix} q_2 \\ q_4 \end{bmatrix} = \begin{bmatrix} 0 & 0 & \frac{I_D + K_A + K_B + K_C}{-J_D \Omega} \\ 1 & 0 & 0 \end{bmatrix} \mathbf{x} \quad (10)$$

where  $\Omega$  is the spin speed of the rotor disk (body D),  $T_2$  is the torque applied through motor 2, and  $I_x, J_x, K_x$  ( $x = A, B, C$  and D) are the scalar moments of inertia about the  $i^{th}$  ( $i=1,2,3$ ) direction respectively in bodies A, B, C and D. Note that this model is valid only for small displacements around the operating point.

## 5 Controller Design

Following the procedure outlined previously, first a nominal controller  $K_0$  is obtained using (10) as a plant model. Hence, the nominal plant  $P_0$  is given by

$$P_0 = \frac{1}{s(s^2 + 389.2)} \begin{bmatrix} 10.33s \\ -38.69 \end{bmatrix} \quad (11)$$

where the open-loop poles are located at 0 and  $\pm 19.729j$ . Hence  $P_0$  has all its poles on the imaginary axis. Consequently,  $P_0 \notin H_\infty$ . A high-gain observer-based controller is designed such that the closed-loop poles are located at

$$\text{State Feedback} \begin{cases} -10 \pm 40j \\ -30 \end{cases} \quad \text{Observer} \begin{cases} -35 \\ -36 \\ -37 \end{cases}$$

This controller results in a fairly fast response with a small overshoot while keeping the controlling voltage between the limits of the saturation. In the next step of the GIMC controller design, the robustness controller  $Q$  is designed to tolerate sensor faults as presented in (1). In this way, sensor faults are modeled by uncertainty in the output signal. This uncertainty representation can also be viewed as output multiplicative uncertainty. Next, the system is put in the standard LFT framework by using (9). Consequently,  $Q$  is chosen according with the following optimization criterion (robust-stabilization)  $\gamma = \min_Q \|\mathcal{F}_l(G, Q)\|_\infty$ .

As a result, the optimization scheme gives a controller  $Q$  with  $\gamma = 1.0$ , this value is expected since this represents that the complete sensors outage cannot be tolerated. For comparison an  $H_\infty$  controller is designed based also on measurement uncertainty. However, in order to make the  $H_\infty$  formulation well-posed, a small penalty  $\epsilon$  is imposed on the control signal. Thus, the following optimization problem is formulated

$$\gamma = \min_{K_\infty} \|\mathcal{F}_l(G, K_\infty)\|_\infty \quad \text{where} \quad G = \begin{bmatrix} 0 & P_0 \\ 0 & \epsilon \\ I & P_0 \end{bmatrix}$$

Like in the GIMC controller, the resulting  $H_\infty$  controller  $K_\infty(s)$  gives again  $\gamma = 1.0$ . Finally, the performance of the three controllers  $K_0, K_\infty$  and *GIMC* are investigated. In this feedback

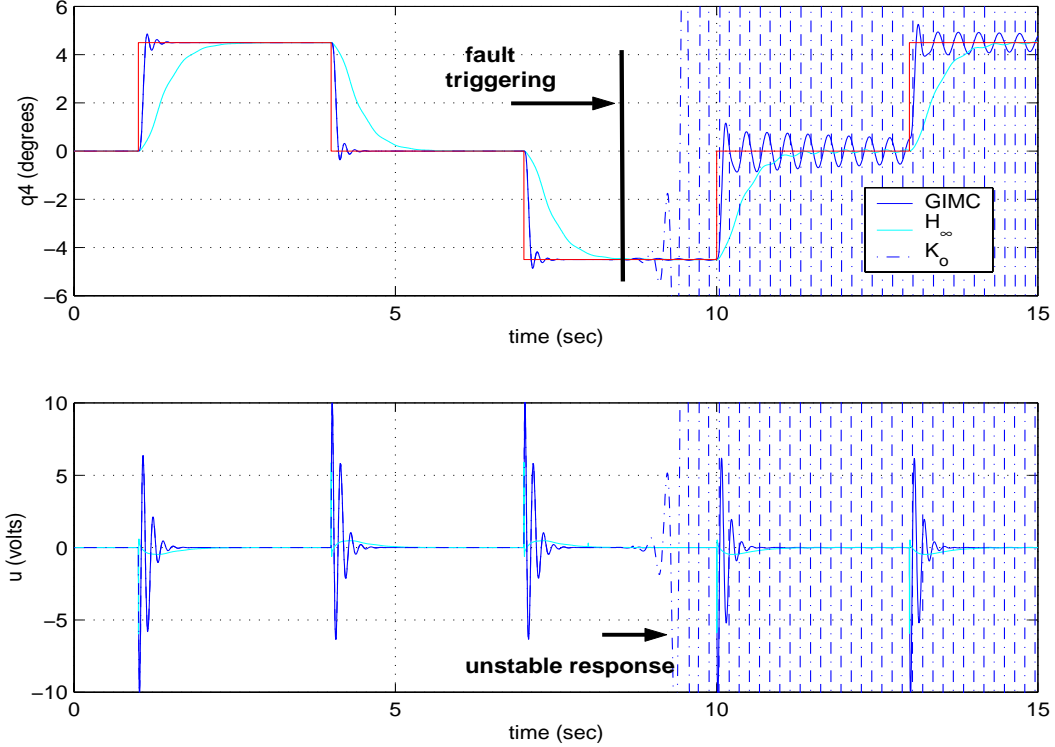


Figure 6: Simulation with sensor fault at 8 sec.

configuration, there are two sensor measurements  $q_2$  and  $q_4$  (Axes 2 and 4). We consider the case when there is a sensor outage of Axis 2, i.e

$$\hat{q}_2(t) = \begin{cases} q_2(t) & t < t_0 \\ 0 & t \geq t_0 \end{cases}$$

where  $\hat{q}_2(t)$  represents the measurement,  $q_2(t)$  the true reading and  $t_0$  the failure time. Thus, the simulation of the response to a square wave reference signal is computed with sensor fault in Axis 2 ( $q_2$ ) at  $t_0 = 8$  sec as shown in Figure 6.

From these plots, it is seen that the system with the nominal controller becomes unstable in the event of sensor fault. On the other hand, the systems with  $H_\infty$  and  $GIMC$  controllers remain stable. It can also be seen that the system response with the  $H_\infty$  controller is not clearly affected by the sensor fault, but the drawback is its slow response. As expected, the system with the  $GIMC$  controller keeps the performance of the nominal controller in the case of no fault, but in the case of fault, it still maintains stability with reasonable tracking.

In addition, these controllers are also tested experimentally. The responses to a square wave command signal (without fault) are shown in Figure 7. The results present a peculiar behavior of the experimental configuration. While the rotor is spinning, the control signal applies an input voltage to motor #2 in order to rotate this gimbal, which produces a corresponding angular velocity in the gimbal #4 ( $q_4$ ) direction. But due to friction mainly, small displacements of gimbal #2 ( $q_2$ ) do not produce any motion in Axis 4. This behavior could be characterized by a dead-zone nonlinearity, but it is more complicated than that. Because, it is not coming from the dc-motor characteristics, instead it is related to interactions among gyroscope components. Consequently, the  $H_\infty$  controller



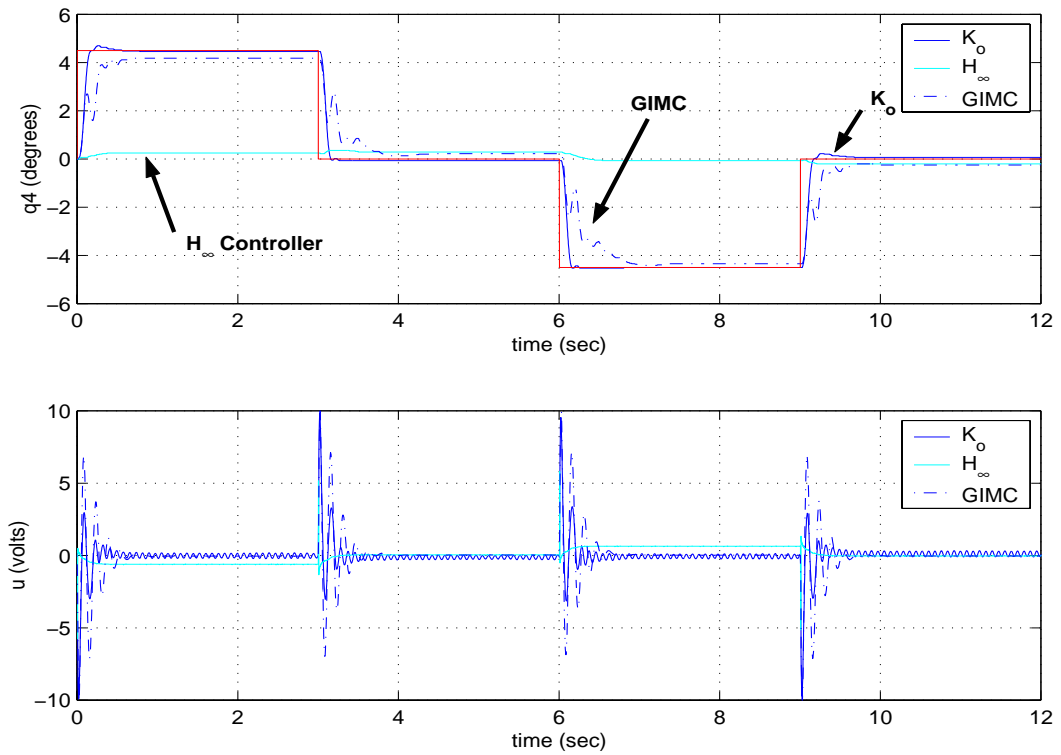


Figure 7: Experimental responses without fault.

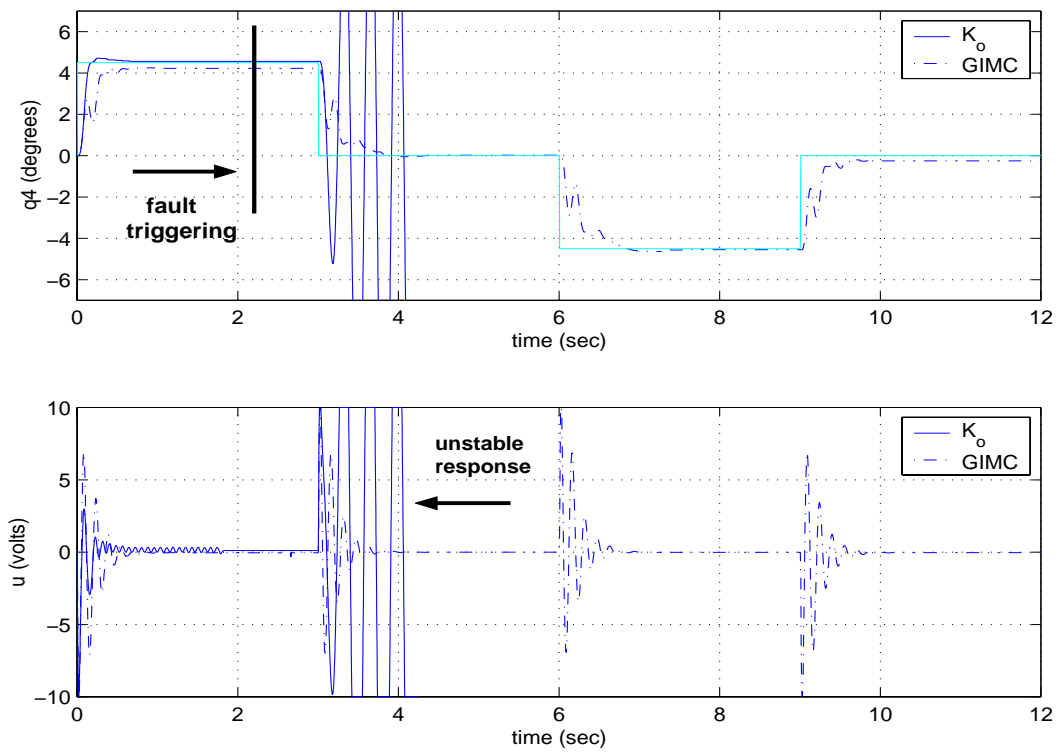


Figure 8: Experimental response with sensor fault at 2.2 sec.

response is drastically affected, since almost no movement in the Axis 4 direction is detected, producing a useless controller.

Meanwhile, the experimental response of the nominal controller  $K_0$  is not much different from the simulation due to the high gain of this controller. On the other hand, the response with the *GIMC* controller is affected since there is large error between the model and true system. Nevertheless, the system with this controller still maintains good tracking.

Finally, the experimental response with fault in Axis 2 ( $q_2$ ) sensor is tested. The fault is programmed at 2.2 seconds, i.e. the reading from that sensor is switched off after 2.2 seconds. No external disturbances are considered during testing. The results are shown in Figure 8. The plot shows how the nominal controller  $K_0$  immediately produces an unstable response, as predicted by simulation. Now, the real advantage of the *GIMC* architecture is obvious: even in the case of sensor fault (outage) the tracking capabilities are not significantly affected. After the sensor fault,  $q$  tries to compensate the nominal control signal  $\hat{u}$  to preserve stability and to keep the tracking response.

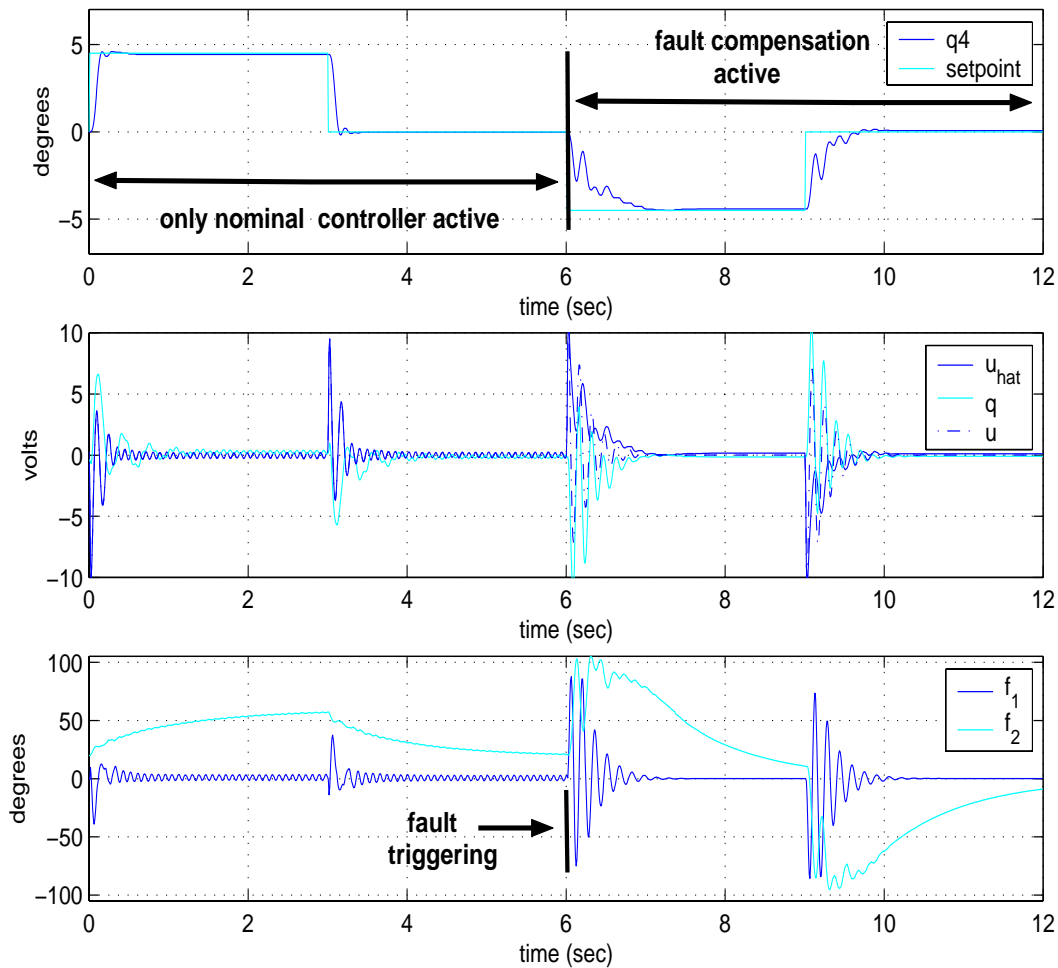


Figure 9: Experimental response: switching on the robustness signal  $q$  after detecting sensor failure (6 sec.).

Now, the idea proposed in Figure 2 is followed. Thus, the robustness loop is switched on only in the case of a sensor failure. The failure condition is then detected by monitoring the signal  $r$

(residual). However, it is needed to choose an strategy to detect a sensor failure from the residual  $r$ . The following simple approach is chosen since external disturbances are not considered, check the standard behavior of this signal for no-failure case and set a threshold value such that if  $r$  goes above it the signal  $q$  is activated. The approach taken is by no means the most efficient way to detect the sensor failure, specially if external disturbances are considered. Other approaches like monitoring the statistics of  $r$  could lead to a more efficient detection. However, only the overall application is intended to be illustrated here. Nevertheless, if external disturbances are considered to influence the system, a detection strategy based on the norm of a weighted residual  $\hat{r}$  over a finite period of time  $T$  [17] can be adopted, i.e.

$$J = \|\hat{r}(t)\|_{2,t,T} = \sqrt{\int_{t-T}^t \hat{r}^T(\tau)\hat{r}(\tau)d\tau} > J_{th} \quad (12)$$

where  $\hat{r}(s) = R(s) [\tilde{N}u(s) - \tilde{M}y(s)]$ ,  $J_{th}$  is a threshold value to prevent false triggering, and  $R(s)$  is a filter chosen to maximize the sensitivity to faults and minimize the effect of disturbances [7].

The fault-tolerant approach is tested in the experimental setup with failure of Axis 2 ( $q_2$ ), sensor outage, after 6 sec as shown in Figure 9. From this plot, it is clear that the controller is able to stabilize the system and achieve good performance even after the failure. Thus, the performance of the GIMC architecture is drastically improved since there is no sacrifice of performance for robustness before the fault.

## 6 Conclusion

The motivation of this work has been to present how the GIMC architecture can be adopted to the fault tolerant control problem in MIMO (Multi-Input Multi-Output) systems. The GIMC architecture is motivated from  $H_\infty$  design and this particular configuration has appealing characteristics for fault-tolerant control. The advantage of this new architecture over standard control is successfully demonstrated on a SITO (Single-Input Two-Output) configuration of a gyroscope system. The classical  $H_\infty$  based controller has shown to be useless in our experiment due to unmodeled nonlinearities in the system. Hence, the GIMC controller is presented as an extension of the  $H_\infty$  technique that overcome the conservativeness of the latter one. Moreover, from the analysis of the properties of the signals in the GIMC architecture, it is possible to derive a reconfigurable control strategy that keeps the nominal performance for no-sensor failure and maintains stability and good tracking in case of a sensor fault in our system.

## References

- [1] S. Altug, M.Y. Chow, H.J. Trussell, "Fuzzy Inference Systems Implemented on Neural Architectures for Motor Fault Detection and Diagnosis," *IEEE Transactions on Industrial Electronics*, Vol. 46, No. 6, pp. 1063-1079, 1999.
- [2] J. Chen and R.J. Patton, *Robust Model-Based Fault Diagnosis for Dynamic Systems*, Kluwer Academic Publishers, 1999.
- [3] L.H. Chiang, E.L. Russell and R.D. Braatz, *Fault Detection and Diagnosis in Industrial Systems*, Springer-Verlag London Limited, 2001.

- [4] E.G. Collins Jr. and T. Song, "Robust  $H_\infty$  Estimation and Fault Detection of Uncertain Dynamic Systems," *Journal of Guidance, Control and Dynamics*, Vol. 23, No. 5, pp. 857-864, 2000.
- [5] C. De Persis and A. Isidori, "A Geometric Approach to Nonlinear Fault Detection and Isolation," *IEEE Transactions on Automatic Control*, vol. 46, No. 6, pp. 853-865, 2001.
- [6] L. Dinca, T. Aldemir and G. Rizzoni, "A Model-Based Probabilistic Approach for Fault Detection and Identification with Application to the Diagnosis of Automotive Engines," *IEEE Transactions on Automatic Control*, Vol. 44, No. 11, pp. 2200-2205, 1999.
- [7] X. Ding, L. Guo and P.M. Frank, "A Frequency Domain Approach to Fault Detection of Uncertain Dynamic Systems", *Proceedings of the 32nd Conference on Decision and Control*, pp. 1722-1727, San Antonio, Texas, December 1993.
- [8] H. Hammouri, M. Kinnaert and E.H. El Yaagoubi, "Observer-Based Approach to Fault Detection and Isolation for Nonlinear Systems," *IEEE Transactions on Automatic Control*, Vol. 44, No. 10, pp. 1879-1884, 1999.
- [9] S.H. Huang, J. Lam, G. Yang, and S. Zhang, "Fault Tolerant Decentralized  $H_\infty$  Control for Symmetric Composite Systems," *IEEE Transactions on Automatic Control*, Vol. 44, No. 11, pp. 2108-2114, 1999.
- [10] D. Kim and Y. Kim, "Robust Variable Structure Controller Design for Fault Tolerant Flight Control," *Journal of Guidance, Control and Dynamics*, Vol. 23, No. 3, pp. 430-437, 2000.
- [11] H. Noura, D. Sauter, F. Hamelin and D. Theilliol, "Fault-Tolerant Control in Dynamic Systems: Application to a Winding Machine," *IEEE Control Systems Magazine*, Vol. 20, No. 1, pp. 33-49, 2000.
- [12] Z. Qiu and J. Gertler, "Robust FDI Systems and  $H_\infty$  Optimization," *Proceedings of the 32nd Conference on Decision and Control*, pp. 1710-1715, San Antonio, Texas, December 1993.
- [13] D. Sauter and F. Hamelin, "Frequency-Domain Optimization for Robust Fault Detection and Isolation in Dynamic Systems," *IEEE Transactions on Automatic Control*, Vol. 44, No. 4, pp. 878-882, 1999.
- [14] L.C. Shen, S.K. Chang and P.L. Hsu, "Robust Fault Detection and Isolation with Unstructured Uncertainty Using Eigenstructure Assignment," *Journal of Guidance, Control and Dynamics*, Vol. 21, No. 1, pp. 50-57, 1998.
- [15] G. Tao, S. Chen and S.M. Joshi, "An Adaptive Actuator Failure Compensation Controller Using Output Feedback," *IEEE Transactions on Automatic Control*, Vol. 47, No. 3, pp. 506-511, 2002.
- [16] Z. Yang and J. Stoustrup, "Robust Reconfigurable Control for Parametric and Additive Faults with FDI Uncertainties," *Proceedings of the 39th Conference on Decision and Control*, Sydney, Australia, December 2000.
- [17] H. Ye, S.X. Ding and G. Wang, "Integrated Design for Fault detection Systems in Time-Frequency Domain," *IEEE Transactions on Automatic Control*, Vol. 47, No. 2, pp. 384-390, 2002.

- [18] K. Zhou and Z. Ren, "A New Controller Architecture for High Performance, Robust and Fault Tolerant Control," *IEEE Transactions on Automatic Control*, Vol. 46, No.10, pp. 1613-1618, 2001.
- [19] K. Zhou, J.C. Doyle and K. Glover, *Robust and Optimal Control*. Prentice Hall, Upper Saddle River, New Jersey, 1996.